

One neutron photoemission cross section of ^{238}U

F. Gerab and M. N. Martins

*Laboratório do Acelerador Linear, Instituto de Física, Universidade de São Paulo,
C.P. 20516, 01498-970 São Paulo, São Paulo, Brazil*

(Received 8 December 1992)

The (e, n) cross section and the $(e + \gamma, n)$ yield have been measured for ^{238}U in the electron energy range 12–60 MeV. The experimental results have been analyzed using distorted-wave Born approximation $E1$ and $E2$ virtual photon spectra for a finite nucleus in order to derive the $E1$ and $E2$ components of the (γ, n) cross section. The $E1$ component exhausts 40% of the $E1$ energy weighted sum rule while the isoscalar $E2$ exhausts 70–80 % of its sum.

PACS number(s): 24.30.Cz, 25.20. - x

I. INTRODUCTION

The decay of the isoscalar electric quadrupole resonance (IS $E2$) in ^{238}U has been extensively studied by means of several experiments using different methods, [1–4] but a few points still remain unclear. The integrated isoscalar $E2$ strength present in the two open channels (fission and one neutron emission) is below the expected value of about one $E2$ sum rule. The electron scattering coincidence $(e, e'f)$ experiments, by far the more sophisticated ones, are unfortunately subject to ambiguities in the separation of $E2$ and $E0$ components. The largest set of results comes from inclusive experiments, namely disintegration or fission induced by electrons or positrons, using the virtual photon analysis to derive the photonuclear cross sections [2–4]. It is important to notice that all the available data were analyzed using virtual photon spectra (VPS) calculated in DWBA (distorted-wave Born approximation) for a point nucleus or using *ad hoc* corrections for nuclear size effects based on plane-wave Born approximation models. The DWBA calculation for a finite nucleus from Zamani-Noor and Onley [5] has been shown to yield consistent results for heavy nuclei [6]. Since for heavy nuclei the difference between $E2$ spectra for finite and point nuclei is large even for electron energies around 10 MeV, the multipole decomposition performed in these previous experiments must be revised. In this paper we report the measurement of the ^{238}U (e, n) cross section, between 12 and 60 MeV, to extend the energy range of a previous experiment [3]. We also measured the electro-plus-photodisintegration yield (bremsstrahlung induced) to use as an additional constraint on the multipolarity assignments in the analysis. The data were analyzed with the virtual photon technique in order to separate the $E1$ and $E2$ contributions to the (γ, n) channel, using VPS calculated in DWBA for finite nuclei [5].

The experiment was performed using the residual activity technique, thus selecting uniquely the decay channel to be studied. This is one of the few situations where inclusive experiments can have advantage over exclusive ones, since $(e, e'n)$ measurements have severe difficulties in separating the neutrons arising from different channels (αn , fission, fission products, etc.).

II. THE EXPERIMENT

The experiment was performed using the 60 MeV linear electron accelerator of the University of São Paulo. The electrodisintegration cross sections and the electro-plus-photodisintegration yields were obtained by bombarding very thin uranium targets (typically $150 \mu\text{g}/\text{cm}^2$ of ^{238}U) placed in a vacuum chamber and measuring, off line, their residual activity. The charge was integrated by a Faraday cup for the electrodisintegration measurements and a secondary emission monitor (calibrated to the Faraday cup) for the radiator-in measurements.

The cross section was obtained by measuring the activity of the 59.54 keV gamma-ray line from the 6.75 day β^- decay of ^{237}U , using a HPGe low energy photon spectrometer system. The detector efficiency was measured with a ^{241}Am calibrated gamma-ray source [7] in the same fixed geometry used to detect gamma rays from the targets. Since the 59.54 keV level of ^{237}Np is populated from both decays (^{237}U by β^- and ^{241}Am by α emission) with the same branching ratio, our efficiency measurement actually determined the product of the detector efficiency by the solid angle and the 59.54 keV gamma-ray line intensity, thus avoiding several sources of uncertainties. The data acquisition system consisted of an amplifier, an analog-to-digital converter, and a computer-aided measurement and control system connected to a PDP 11/84 computer.

In order to allow enough time for the activity of ^{237}U to die out, measurements were carried out using six UO_3 targets. For the activation of electro-plus-photodisintegration yields a tantalum radiator with $275 \text{mg}/\text{cm}^2$ was placed in the electron beam immediately ahead of the target.

The electrodisintegration results are shown in Fig. 1 by the full circles. The open circles are the results of a previous experiment by Martins *et al.* [3]. This data set had its energy scale corrected due to a small change in the energy calibration function of the São Paulo linac performed in 1979. After this correction the two data sets agree within 4% without any difference in shape. So, after normalization, the old data were used in the analysis in order to complete the low energy region. Also shown in Fig. 1 (by the triangles) are the (e, n) data of Shotter

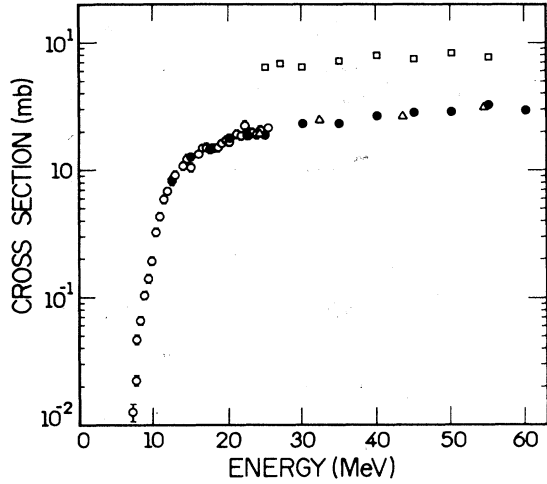


FIG. 1. Electrodisintegration cross sections: Martins *et al.* [3] (open circles), Shotter *et al.* [8] (triangles), this work (full circles). Electro-plus-photodisintegration yield: this work (squares).

et al. [8], without normalization. The electro-plus-photodisintegration data are also shown in Fig. 1 by the squares. The lowest energy point of this data set is at 25 MeV, well above the peak of the photonuclear cross section, so that the correction for energy losses of the beam in the radiator could be done with a very small contribution due to the tip of the spectrum, where the correction by the average energy loss is not valid.

The error bars show the statistical uncertainties when they are larger than the points. The overall uncertainty is 20%.

III. ANALYSIS AND RESULTS

The electrodisintegration cross section $\sigma_{e,x}(E_0)$ may be obtained from the photonuclear cross section $\sigma_{\gamma,x}(E)$ through an integral over the virtual photon intensity spectrum $N^{\lambda L}(E_0, E, Z, A)$:

$$\sigma_{e,x}(E_0) = \int_0^{E_0 - m_e} \sum_{\lambda L} \sigma_{\gamma,x}^{\lambda L}(E) N^{\lambda L}(E_0, E, Z, A) \frac{dE}{E}. \quad (1)$$

In Eq. (1), E_0 stands for the total electron energy and E stands for the energy of the photon of multipolarity λL . In the same spirit, the yield with the radiator is

$$Y_{e,x}(E_0) = \sigma_{e,x}(E_0 - 2\Delta E_0) + N_r \int_0^{E_0 - \Delta E_0 - m_e} \sum_{\lambda L} \sigma_{\gamma,x}^{\lambda L}(E) K(E_0 - \Delta E_0, E) \frac{dE}{E} \quad (2)$$

where N_r is the number of nuclei/cm² in the tantalum radiator, $K(E_0, E)$ is the bremsstrahlung cross section for tantalum, and ΔE_0 is the electron energy loss in half of the radiator thickness.

The cross sections $\sigma_{e,x}(E_0)$ and yields $Y_{e,x}(E_0)$ measured in this work, plus the data of Martins *et al.* [3], shown in Fig. 2, were simultaneously fitted [9] in order to derive the $E1$ and $E2$ photonuclear cross sections. These

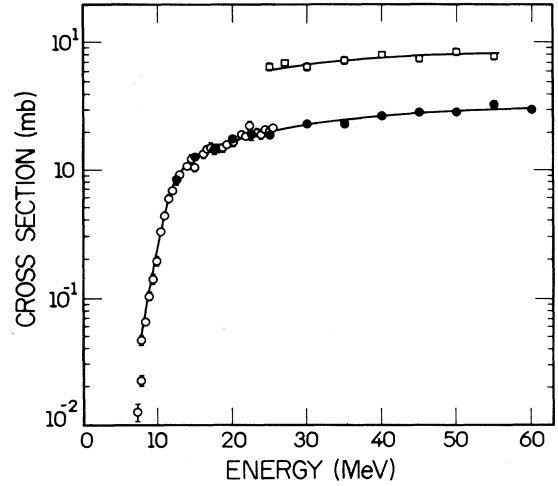


FIG. 2. Electrodisintegration cross sections: Martins *et al.* [3] (open circles); this work (full circles). Electro-plus-photodisintegration yield: this work (squares). The lines represent the fits to the data.

cross sections were represented by coarse histograms, thus not showing any detailed feature of their shapes. The fitting procedure used $E1$ and $E2$ VPS calculated in DWBA for a finite nucleus [5] in Eq. (1) and the bremsstrahlung cross section of Seltzer *et al.* [10] for $K(E_0, E)$ in Eq. (2). The lines shown in Fig. 2 represent the best fit (reduced $\chi^2 = 0.8088$ with 48 degrees of freedom) to the data. The resulting $E1$ and $E2$ cross sections are shown in Fig. 3 by the histograms, the hatched part corresponding to the $E2$ component. The $E1$ component exhausts $(41 \pm 5)\%$ of the $E1$ sum rule, while the $E2$ component exhausts $(86 \pm 22)\%$ of its energy weighted sum rule. It is important to note that, with this method, we are not able

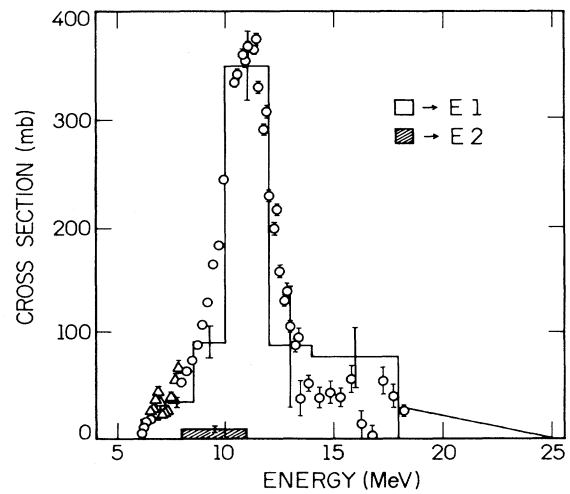


FIG. 3. Photodisintegration cross sections derived by the VIRLIB code: $\sigma_{\gamma,n}^{E1}$ (histogram) and $\sigma_{\gamma,n}^{E2}$ (hatched histogram). Photodisintegration cross sections measured by monochromatic photons: Caldwell *et al.* [12] (open circles) and Dickey and Axel [11] (triangles). There is no normalization between the different sets of data.

to separate isoscalar and isovector $E2$, thus interpreting all the $E2$ strength found as isoscalar. Also shown in Fig. 3 (by the points) is a combination of (γ, n) results obtained from different laboratories using monochromatic photons from positron annihilation in flight. The agreement is quite good and we must emphasize that there is no normalization between the different sets of data.

As an alternate procedure, we analyzed our data employing the (γ, n) cross sections obtained with monochromatic photons as a shape constraint. This was done assuming that the total photodisintegration cross section can be written as $\sigma_{\gamma, n} = \sigma_{\gamma, n}^{E1} + \sigma_{\gamma, n}^{E2(T=0)} + \sigma_{\gamma, n}^{M1}$. So we can rewrite Eq. (1) as

$$\begin{aligned} \sigma_{e, n}(E_0) = & \int_0^{E_0 - m_e} [K_1 \sigma_{\gamma, n}(E) N^{(E1)} \\ & + K_2 \sigma_{\gamma, n}^{E2}(E) (N^{E2} - N^{E1}) \\ & + K_3 \sigma_{\gamma, n}^{M1}(E) (N^{M1} - N^{E1})] \frac{dE}{E}, \end{aligned} \quad (3)$$

where K_i are constants to be determined from the fit. For the $\sigma_{\gamma, n}$ cross section we used a combination of the Dickey and Axel [11] data (between 6.5 and 7.8 MeV) and the Caldwell *et al.* [12] data, in the intervals 6.1–6.4 MeV and 7.9–18.7 MeV. We decided to use the cross section measured in Livermore [12] instead of Saclay [13] because in the work of Wolyneć *et al.* [14] about the differences of the cross sections from these two laboratories, it is shown that the Saclay measurements may have problems in the multiplicity sorting procedure. The (γ, n) cross section was measured up to 18.7 MeV only, so we had to make an *ad hoc* assumption about its behavior above this energy. We made a linear extrapolation, from the average value of 26.5 mb at 18.7 MeV to zero at 25 MeV. This is a reasonable assumption, since the integrated $\sigma_{\gamma, n} + \sigma_{\gamma, pn}$ cross section from 18.3 to 140 MeV should be around 136 mb MeV [15] (which gives an average cross section of 1.1 mb in this region). The combined cross section is shown in Fig. 3.

In Eq. (3), K_1 is called “normalization constant” because it allows to compensate for differences in the absolute scales of the photodisintegration and electrodisintegration cross sections. The value of K_1 is determined independently, by means of Eq. (2) and the radiator-in data:

$$K_1 = \left\langle \frac{Y_{e, n}(E_0) - \sigma_{e, n}(E_0 - 2\Delta E_0)}{N_r \int_0^{E_0 - m_e - \Delta E_0} \sigma_{\gamma, n}(E) K(E_0 - \Delta E_0, E) dE/E} \right\rangle. \quad (4)$$

The average value of K_1 (over all the radiator-in data) is 0.96 ± 0.08 , showing a very good agreement between the sets of data.

To represent the other cross sections in Eq. (3) we followed the systematics of the literature. For the isoscalar $E2$ we used a Lorentz line shape with peak at 10.5 MeV ($E_p = 10.5$ MeV), 3.0 MeV wide and with 8.25 mb at the peak ($\sigma_p = 8.25$ mb), thus exhausting one energy weight-

ed sum rule. By fitting our data with Eq. (3), K_2 then gives the fraction of the energy weighted sum exhausted by the isoscalar $E2$ cross section. For the $M1$ cross section we assumed a uniform strength of 1 mb distributed between 6.1 and 7.1 MeV, since the $M1$ strength, if present, should be distributed over several individual levels.

Fitting our data keeping K_1 fixed at the value determined by Eq. (4), we obtained $K_2 = 0.75 \pm 0.09$ and K_3 compatible with zero, with a reduced χ^2 of 1.159 (with 43 degrees of freedom). The fit is visually identical to the one shown in Fig. 2. As in the previous analysis, any attempts to include an isovector $E2$ component as a free parameter to be determined by the fit had to be given up because they yielded uncertainties larger than the parameters. We decided to estimate an upper limit for the isovector $E2$ component, assuming a Lorentz line shape with peak position at 21.0 MeV and 5.0 MeV wide. To exhaust one isovector $E2$ energy weighted sum, this cross section should have $\sigma_p = 27.9$ mb. This is clearly incompatible with the total $\sigma_{\gamma, n}$ cross section measured with monochromatic photons, which has a strength of 26.5 mb at 18.7 MeV and should be dropping. From our linear extrapolation, at 21 MeV the cross section should be 8.5 mb high. So we tried a fit fixing $\sigma_p^{E2(T=1)} = 5.6$ mb, thus exhausting 20% of the energy weighted sum. In this fit (still keeping $K_1 = 0.96$) we got $K_2 = 0.68 \pm 0.09$ and K_3 again compatible with zero. The reduced χ^2 of the fit was 1.039 with 43 degrees of freedom.

It is reassuring to notice that the isoscalar $E2$ strength determined is not strongly dependent either on the method of analysis or on the presence of an isovector $E2$ component.

Figure 4 summarizes our results for the isoscalar $E2$ resonance and shows a comparison with other results available. Both our results agree well with the strength predicted by the quasiparticle random phase approximation (QRPA) calculation [16] but, as expected, the information on the shape is not very relevant. The QRPA cal-

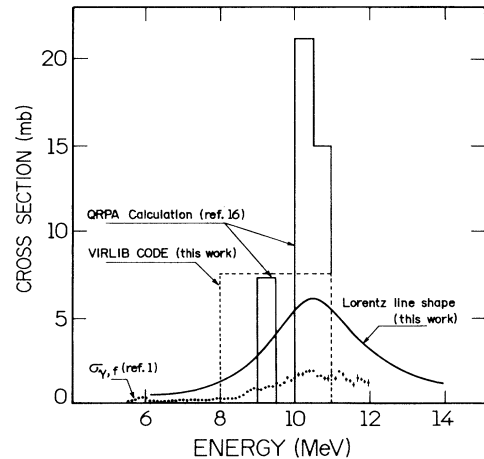


FIG. 4. Isoscalar $E2$ cross sections. QRPA prediction [16] (histogram), $\sigma_{\gamma, f}^{E2}$ [1] (points), $\sigma_{\gamma, n}^{E2}$ derived using the VIRLIB code (this work—dashed histogram), and $\sigma_{\gamma, n}^{E2}$ (Lorentz line shape—this work, see text).

culution, shown by the histogram, exhausts 68.5% of the $E2$ energy weighted sum rule (EWSR), very close to both our results. The points in Fig. 4 represent the $E2$ component of $\sigma_{\gamma,f}$ obtained from the $E2$ strength of Ref. [1]. The transformation of the strength function $dB/d\omega$ to cross section was done by means of the following expression:

$$\sigma(EL, \omega) = \frac{8\pi^3 \alpha}{(\hbar c)^{2L-2}} \frac{(L+1)\omega^{2L-1}}{L[(2L+1)!!]^2} \frac{dB}{d\omega}(EL, \omega),$$

where EL stands for electrical transitions of order L , α is the fine structure constant, \hbar is Planck's constant, and c the velocity of light.

Our results corroborate the $E2/E0$ strength separation for ^{238}U suggested by the authors of Ref. [1]. They suggested that the $E2$ component should dominate the strength distribution up to 12 MeV, with an integrated strength exhausting $(19 \pm 2)\%$ of the $E2$ EWSR. Our result with the Lorentz line shape exhausts $(75 \pm 9)\%$ of the $E2$ EWSR, meaning that the two dominant decay channels (fission and one neutron emission) exhaust $(94 \pm 9)\%$ of the $E2$ EWSR, very close to the total exhaustion expected in this mass region.

IV. CONCLUSIONS

The absolute cross sections for one neutron emission by absorption of real and virtual photons have been measured in ^{238}U up to 60 MeV. The $E1$ and $E2$ photonuclear cross sections have been derived from these data. The multipole decomposition was done by two different

methods, yielding compatible results.

The one neutron emission channel is the dominant decay mode for the isoscalar $E2$ resonance, exhausting around 70–80% of the energy weighted $E2$ sum rule. The $E1$ component decaying through this channel exhausts 40% of its sum. Our analysis procedure was unable to detect any $M1$ contribution to the cross section and could only define an upper limit for the isovector $E2$ component of about 20% of its energy weighted sum.

The experimental results obtained in this work are in good agreement with previous measurements, but the photonuclear cross sections derived from them changed somewhat due to the use of virtual photon spectra calculated for finite size nuclei in the analysis. Our results, together with the results for the fission channel available from the literature, indicate that the two dominant channels for the decay of the isoscalar $E2$ resonance (fission and one neutron emission) exhaust about 90–100% of the $E2$ sum, as expected.

ACKNOWLEDGMENTS

The authors wish to thank Dr. David Onley for supplying the code for computing DWBA virtual photon spectra for finite nuclei that made the analysis possible. We appreciated very much all the critical comments provided by Prof. J. D. T. Arruda-Neto. We would like to acknowledge the support of FAPESP (Fundação de Amparo à Pesquisa do Estado de São Paulo) and CNPq (Conselho Nacional de Desenvolvimento Científico e Tecnológico).

-
- [1] Th. Weber, R. D. Heil, U. Kneissl, W. Wilke, Th. Kihm, K. T. Knöpfle, and H. J. Emrich, Nucl. Phys. **A510**, 1 (1990), and references therein.
- [2] J. D. T. Arruda-Neto, S. B. Herdade, B. S. Bhandari, and I. C. Nascimento, Phys. Rev. C **18**, 863 (1978).
- [3] M. N. Martins, E. Wolyneec, and G. Moscati, Phys. Rev. C **16**, 613 (1977).
- [4] H. Ströher, R. D. Fischer, J. Drexler, K. Huber, U. Kneissl, R. Ratzek, H. Ries, W. Wilke, and H. J. Maier, Phys. Rev. Lett. **47**, 318 (1981).
- [5] F. Zamani-Noor, Ph.D. thesis, Ohio University, 1984 (unpublished); F. Zamani-Noor and D. S. Onley, Phys. Rev. C **33**, 1354 (1986).
- [6] E. Wolyneec, V. A. Serrão, and M. N. Martins, J. Phys. G **13**, 515 (1987).
- [7] Calibrated ^{241}Am source (source 7Q272) manufactured by Amersham International Limited.
- [8] A. C. Shotter, C. H. Zimmerman, J. M. Reid, J. C. McGeorge, and A. G. Flowers, Nucl. Phys. **A330**, 325 (1979).
- [9] Code VIRLIB is a modified version of code VIRLIN, developed by R. G. Leicht. The changes were done by P. Gouffon and M. N. Martins.
- [10] S. M. Seltzer and M. J. Berger, Nucl. Instrum. Methods B **12**, 95 (1985).
- [11] P. A. Dickey and P. Axel, Phys. Rev. Lett. **35**, 501 (1975).
- [12] J. T. Caldwell, E. J. Dowdy, B. L. Berman, R. A. Alvarez, and P. Meyer, Phys. Rev. C **21**, 1215 (1980).
- [13] A. Veyssièrè, H. Beil, R. Bergère, P. Carlos, A. Leprêtre, and K. Kernbath, Nucl. Phys. **A199**, 45 (1973).
- [14] E. Wolyneec, A. R. V. Martinez, P. Gouffon, Y. Miyao, V. A. Serrão, and M. N. Martins, Phys. Rev. C **29**, 1137 (1984).
- [15] A. Leprêtre, H. Beil, R. Bergère, P. Carlos, J. Fagot, A. De Miniac, and A. Veyssièrè, Nucl. Phys. **A367**, 237 (1981).
- [16] D. Zawischa and J. Speth, in *Proceedings of the International Symposium on Nuclear Fission and Related Collective Phenomena and Properties of Heavy Nuclei*, Bad Honnef, Germany, 1981, edited by P. David, T. Mayer-Kuckuk, and A. van der Woude, Lecture Notes in Physics Vol. 158 (Springer-Verlag, Berlin, 1982), p. 231.